Soft Matter

PAPER

View Article Online
View Journal | View Issue

Cite this: *Soft Matter*, 2023, **19**, 8507

The effect of polymer end-group on the formation of styrene – maleic acid lipid particles (SMALPs)†

George M. Neville, [ab] Kerrie A. Morrison,[ac] Ella R. Shilliday,[b] James Doutch,[d] Robert Dalgliesh,[d] Gareth J. Price [be] and Karen J. Edler [‡*ac]

A series of block copolymers comprising styrene and maleic acid (SMA) has been prepared using RAFT polymerisation. RAFT often results in a large hydrophobic alkylthiocarbonylthio end group and this work examines its effect on the solution behaviour of the copolymers. SMA variants with, and without, this end group were synthesised and their behaviour compared with a commercially-available random copolymer of similar molecular weight. Dynamic light scattering and surface tension measurements found the RAFT-copolymers preferentially self-assembled into higher-order aggregates in aqueous solution. Small angle neutron scattering using deuterated styrene varients add support to the accepted model that these agreggates comprise a solvent-protected styrenic core with an acid-rich shell. Replacing the hydrophobic RAFT end group with a more hydrophilic nitrile caused differences in the resulting surface activity, attributed to the ability of the adjoining styrene homoblock to drive aggregation. Each of the copolymers formed SMALP nanodiscs with DMPC lipids, which were found to encapsulate a model membrane protein, gramicidin. However, end group variation affected solubilisition of DPPC, a lipid with a higher phase transition temperature. When using RAFT-copolymers terminated with a hydrophobic group, swelling of the bilayer and greater penetration of the homoblock into the nanodisc core occurred with increasing homoblock length. Conversely, commercial and nitrile-terminated RAFT-copolymers produced nanodisc sizes that stayed constant, instead indicating interaction at the edge of the lipid patch. The results highlight how even minor changes to the copolymer can modify the amphiphilic balance between regions, knowledge useful towards optimising copolymer structure to enhance and control nanodisc formation.

Received 3rd September 2023,
Accepted 22nd October 2023

DOI: 10.1039/d3sm01180a

rsc.li/soft-matter-journal

Introduction

Membrane proteins, MPs, are vital components of the structural and functional properties of biological cells[1] and are the key to many drug treatments. Some time ago it was suggested that MPs comprise around 70% of pharmaceutical targets.[2,3] An understanding of the structure of MPs is therefore crucial to developing healthcare technologies, both diagnostic and therapeutic, as well as for developing new agrochemicals such as target-specific pesticides.

Despite their importance, surprisingly little progress has been made in elucidating the structure, dynamics and function of MPs. For example, such proteins account for only a small fraction of all high resolution structures in the Protein Data Bank.[4] This is due in large part to the difficulty of obtaining the protein in its native state which is often heavily reliant on preserving the surrounding lipid environment. The amphiphilic nature of this environment, upon which the structural integrity and function of MPs depend, precludes direct solubility in water in an unaltered state[5,6] making their extraction and purification particularly challenging.

A common method to purify MPs has been to use detergents where MPs can be stabilised in self-assembled surfactant micelles.[3,7] However, although a number of useful systems have been developed,[8] detergent micelles are a poor model for cell membranes so the MPs often denature or undergo structural reorganisation during extraction. Detailed studies have therefore

[a] *Centre for Sustainable Chemical Technologies, University of Bath, Claverton Down, Bath, BA2 7AY, UK. E-mail: karen.edler@chem.lu.se*
[b] *Department of Chemistry, University of Bath, Claverton Down, Bath BA2 7AY, UK*
[c] *Department of Life Sciences, University of Bath, Claverton Down, Bath BA2 7AY, UK*
[d] *ISIS Pulsed Neutron and Muon Source, Rutherford Appleton Laboratory, Didcot, OX11 0QX, UK*
[e] *Department of Chemistry, Khalifa University, P.O. Box 127788, Abu Dhabi, United Arab Emirates*

† Electronic supplementary information (ESI) available: Polymer synthesis, polymer characterisation, solution behaviour and SANS. See DOI: https://doi.org/10.1039/d3sm01180a

‡ Present address: Department of Chemistry, Centre for Analysis and Synthesis, Lund University, PO Box 124, SE-221 00.

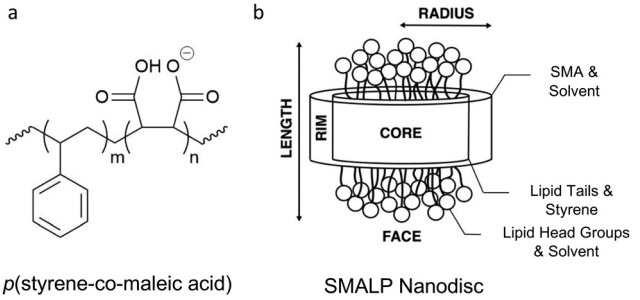

Fig. 1 (a) Chemical structure of poly(styrene-*co*-maleic acid) partially deprotonated at operational pH 7–9. (b) Schematic representation of SMALP nanodisc, which defines terms and components used in fitting the SANS data below to a core shell bicelle model.

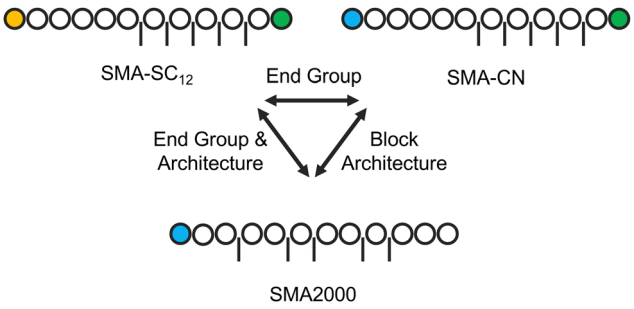

Fig. 2 Structural styrene (circles) maleic acid (bars) copolymer representations emphasising the comparisons between variants with similar molecular weights: Commercial SMA2000 with random architecture, RAFT-made SMA with block architecture and a hydrophobic SC_{12} end group (orange circles) and hydrophilic COOH group (green circles), and RAFT-made SMA with an altered hydrophilic CN end group (blue circles).

been limited to those MPs extractable in their active folded-form. While alternatives to this approach have been developed,[9,10] none has managed to entirely exclude detergents from work-up, nor to retain native phospholipid bilayer environments.

Considerable progress in studying MPs has been facilitated by the discovery[11] that amphiphilic copolymers based on styrene (St) and maleic acid (MA) are able to extract MPs complete with their proximal lipids, stabilising them in water without the need to employ detergents. The copolymers (Fig. 1a) exploit a balance between hydrophobic regions provided by styrene which interact with the lipid tails, and charged hydrophilic regions from MA which provide water stability to form self-assembled 'nanodiscs' (Fig. 1b), coined 'styrene maleic acid lipid particles' or 'SMALP's. Direct extraction of MPs and lipids from cells is possible *via* the insertion of the copolymer into the cell membrane with the styrene rings intercalating into the lipid tails and the MA groups allowing hydrogen bonding and ionic interactions with the aqueous solvent.[12–15] SMA copolymers are produced by a reaction between styrene with maleic anhydride, MAnh, the relative reactivities of which mean that they generally form alternating copolymers.[16] The anhydride can then be readily hydrolysed to the acid form.[17] A range of copolymers is available commercially with varying molecular weights and, by exploiting feed-starved polymerisations, varying St : MA ratios. It has generally been found that whether SMALPs can be formed does not depend to any great extent on molecular weight but is heavily influenced by St : MA ratio, values around 2 : 1 or 3 : 1 usually being the most effective.[13,18] While SMA copolymers dominate published studies, the copolymers are effective only over a narrow pH range (7–9) and are sensitive to small concentrations of divalent cations. Several structural variants[13] of SMA as well as a small number of other copolymers[19–21] have been found to produce SMALP-like nanodiscs, although only a few workable copolymer variants have been widely exploited thus far.

While structural investigations have provided strong evidence for the model morphology shown in Fig. 1b,[12] there is still some doubt and discussion about the precise mode of action of the copolymers. Detailed studies have largely used commercially available variants of the copolymers and interpretation of observations is hampered by their polydisperse nature, in both composition and chain length. To simplify the discussion, Hall *et al.*,[22] Harding *et al.*[23] and Craig *et al.*[24] among others such as Klumperman,[25] have used the RAFT method of controlled radical polymerisation to produce copolymers with a precisely known chain architecture and narrow distribution of chain lengths. These polymerisations usually produce a diblock material consisting of a block of alternating St:MA with a tail block of homo-styrene compared with the more random structure of the commercial materials (Fig. 2). This leads to differences in the SMALP size when the different polymers are used.[22]

Another consequence of using the RAFT method is that, in addition to the diblock architecture, the copolymer carries an inherently hydrophobic alkylthiocarbonylthio end group. The nature of the alkyl group depends on the RAFT agent used; often this is a $C_{12}H_{25}$ group. However, the effects of this large end group in terms of its influence on nanodisc formation have yet to receive attention. The aim of the work reported here is to prepare SMA copolymers with and without the hydrophobic end group and to compare their behaviour with a commercial SMA copolymer with similar overall composition and chain length (Fig. 2). The nature of the structures formed by the SMA copolymers in solution has also been investigated using small angle neutron scattering (SANS).

Experimental

Polymer synthesis & characterisation

Materials. Before polymerisation, styrene (*Merck*, purity ≥ 99%), was passed through a disposable, pre-packed column (*Merck*) to remove the inhibitor 4-*tert*-butylcatechol. The comonomer, maleic anhydride (MAnh) (puriss, purity ≥ 99%), the initiator, 2,2′-Azobis(2-methylpropionitrile) (AIBN), the RAFT agent, 2-(dodecylthiocarbonothioylthio)-2-methylpropionic acid (DDMAT) (purity 98%, HPLC grade), and the solvent, 1,4-dioxane were purchased from *Merck* and were used as received. The commercial SMA variant, SMA2000, was provided by *Cray Valley*. The lipids, *t*-2-dimystoyl-*sn*-glycero-3-phosphocholine (DMPC) (purity ≥ 99%), 1,2-dipalmitoyl-*sn*-glycero-3-phosphocholine (DPPC) (purity ≥ 99%) and gramicidin (from Bacillus Aneurinolyticus) were purchased from *Merck*, and deuterated 1,2-dimyristoyl-d54-*sn*-glycero-3-phosphocholine (d-DMPC) (purity > 99%) from *Avanti Polar*

Lipids. Lauroyl peroxide (LPO) was purchased from *BDH Chemicals LTD*, and mono and dibasic sodium phosphate (purity ≥ 99%) from *Acros Organics*. All other solvents used were purchased from *Merck* and used as received.

Reversable-addition–fragmentation-chain transfer (RAFT) copolymerisation of SMAnh. Copolymers were synthesised using the RAFT method as described previously[22] based on the method of Harrison and Wooley.[26] Briefly, the relevant masses of styrene and MAnh were dissolved in a small amount of dioxane with AIBN initiator and 2-(dodecylthiocarbonothioylthio)-2-methylpropionic acid (DDMAT) as the RAFT agent (Scheme 1: full experimental details given in ESI†). Reaction mixtures were then sealed in round bottom flasks before three freeze–thaw cycles under vacuum, prior to polymerisation at 60 °C for 24 hours. The copolymer was recovered by precipitation in ice-cold diethyl ether.

End group modification of SMAnh-SC_{12} to SMAnh-CN. RAFT polymerisations result in a polymer end group dependent on the RAFT agent used. Here, this is dodecylthiocarbonothioylthio which is hydrophobic (coded SMAnh-SC_{12}). Modification of this end group to a hydrophilic cyanoisopropyl group (coded SMAnh-CN) followed the method of Chen *et al.*,[27] as outlined in Scheme S1 (ESI†). An excess of radical initiators, AIBN (20 molar equivalents) and lauroyl peroxide (LPO) (2 molar equivalents) was added to a 3% (wt/v) polymer solution in toluene. This was then degassed with nitrogen followed by three freeze–thaw cycles to exclude oxygen, before being heated to 80 °C for 4 hours. The solution was then dried under nitrogen before hydrolysis without the need for further modification.

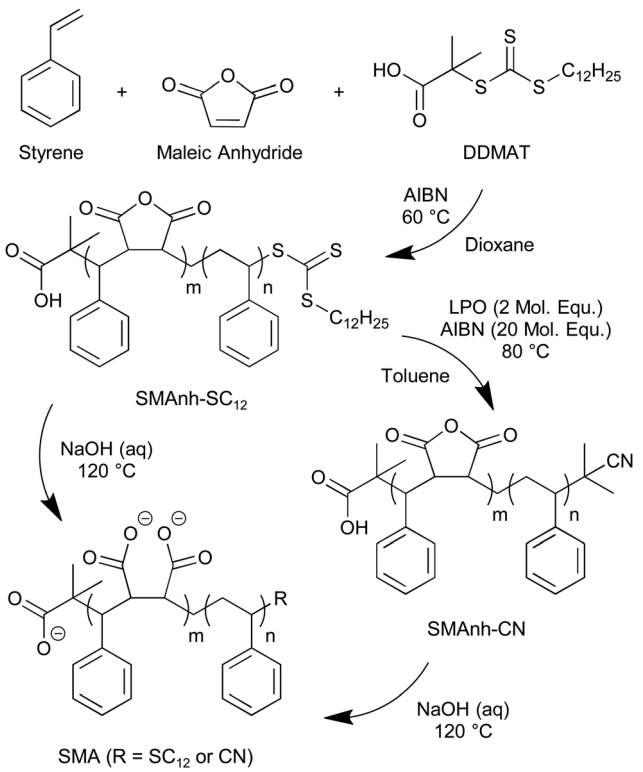

Scheme 1 Reaction scheme for the RAFT synthesis of styrene-maleic anhydride copolymers (SMAnh-SC_{12}), subsequent end group exchange of SMAnh-SC_{12} to SMAnh-CN, and SMA work up by basic hydrolysis.

Hydrolysis of SMAnh to SMA. SMAnh was hydrolysed to SMA in accordance with the procedure outlined by Hall *et al.*,[22] whereby a 10% (wt/v) polymer solution in 1 M aqueous NaOH was heated to 120 °C for 2 hours, under reflux. Polymers were then precipitated by acidification to pH 3 with 4 M aqueous HCl, and centrifugation using an *Eppendorf 5804R* centrifuge for 15 minutes at 21 °C at 8000 rpm. The supernatant was removed and the pellet washed with water and centrifuged again a further three times. To further purify the polymer, the pellet was dissolved in 0.6 M NaOH before repeating the precipitation and washing procedure. The precipitate was then dissolved in 0.6 M NaOH and adjusted to pH 8.0, to ensure sufficient deprotonation of MA moieties for nanodisc formation, before freeze drying (*Virtis SP Scientific*) for a minimum of 24 hours.

UV-vis spectroscopy. Spectra of aqueous SMA solutions in PBS buffer solution were recorded using an *Agilent Cary 60* UV-vis spectrometer and a quartz cuvette. To estimate the percentage end group conversion, resultant spectra were normalised by the styrenic absorbance peak at 260 nm, the concentration of which is unchanged by end group conversion. This can then be compared to the spectrum for a solution of SMA2000, which has no thiocarbonylthio end groups.

Fourier-transform-infrared (FTIR) spectroscopy. FTIR conducted on a *PerkinElmer* ATR desktop spectrometer with solid-state polymer samples at room temperature using 16 scans with a resolution of 1 cm^{-1}.

^{1}H & ^{13}C nuclear magnetic resonance (NMR) spectroscopy. ^{1}H NMR spectra were recorded using an *Agilent* 500 MHz NMR spectrometer. SMAnh and SMA polymers were dissolved in d_6-acetone and D_2O, respectively, at room temperature, at high concentrations (40 mg mL^{-1}). Spectra were processed in *Mestrelab MNova* 11.0 software, where spectra were baseline corrected to allow integration of peak area, and line broadening was systematically employed to ease analysis. ^{13}C spectra were conducted with the same method but lengthened acquisition times to improve signal-to-noise ratios.

Diffusion-ordered spectroscopy (DOSY) ^{1}H NMR spectroscopy. DOSY spectroscopy was conducted on a *Bruker AV* 500 MHz spectrometer at room temperature with anhydride polymer samples dissolved in d_6-acetone (20 mg mL^{-1}). Diffusion coefficients were estimated using eight gradient steps.

Gel permeation chromatography (GPC). SMAnh copolymer molecular weights were estimated by GPC using an *Agilent GPC 1260 Infinity* chromatograph using two PLgel 5 μM MIXED-D 30 cm × 7.5 mm columns with a guard column PLgel 5 μm MIXED Guard 50 × 7.5 mm. The column oven was maintained at 35 °C, with GPC-grade THF as the eluent at a flow rate of 1.00 mL min^{-1} and refractive index detection and polymer concentrations between 1.0–2.0 mg mL^{-1}. The system was calibrated against 12 narrow molecular weight polystyrene standards with a range of M_w from 1050 Da to 2650 kDa. Chromatograms were subsequently analysed in *Agilent GPC/SEC* software to extract M_n and PDI values.

Solution behaviour & structural characterisation. A 50 mM phosphate buffer solution (PBS) was made by mixing 0.1 M

aqueous solutions of monobasic sodium phosphate (2.65 mL, 0.265 × 10 mmol) and dibasic sodium phosphate (47.35 mL, 4.735 mmol), and diluting to 100 mL with 18.2 ΩM ultra-filtered water. NaCl (1.1688 g, 0.02 mol) was then added, resulting in a 0.2 M salt concentration. This produces a PBS stabilised at pH 8.0.

Nanodisc preparation. Nanodiscs were prepared in 50 mM (0.2 M NaCl) PBS stabilised at pH 8.0, within the range nanodiscs may form. Lipid species (5.0 mg), whether DMPC, d-DMPC, or DPPC, were dissolved in 0.679 mL PBS and sonicated in two 10 second bursts, with a 50% duty cycle, separated by a 15 second rest period to prevent overheating. 15 mg of copolymer in 0.231 mL PBS were then added to this solution, resulting in a nanodisc solution consisting of 1.65% (wt/v) copolymer and 0.55% (wt/v) lipid. An immediate indication of successful nanodisc formation arises from the loss of turbidity upon the addition of copolymer.

The model MP, gramicidin, was incorporated from vesicles prepared by a thin film methodology. First, DMPC lipids (5.0 mg) were dissolved in minimal (<1 mL) 1 : 1 chloroform:methanol and gramicidin (0.4 mg) in minimal methanol, before mixing. A few drops of chloroform were added before rotary evaporation at 40 °C until only a residual film remained. This was then swelled with 1 mL PBS at 30 °C and briefly vortexed. The homogenous suspension was then sonicated prior to use as described above.

Pendant drop tensiometry

Tensiometry was conducted on a FTA1000 contact angle/surface tension analyser and processed using *FTA 32* surface tension image analysis software. Syringe needles were prepared by extensive washing with water, ethanol and acetone to remove contaminants. Samples containing SMA polymers in solution at relevant concentrations in PBS were then passed through these needles to produce a small hanging droplet which was imaged at a typical rate of 10 images per second for 10 seconds to ensure a good average measurement (Fig. S5a, ESI†). In the case of dodecane to PBS measurements, the sample drop was suspended in a cuvette of dodecane, utilising a straight needle.

The shape of the droplet and difference in density between the light and heavy phases (Table S2, ESI†) are then used in an iterative convergence calculation to fit eqn (S1) (full description in ESI†). The software was calibrated against 18.2 MΩ ultra-filtered water with a surface tension of 72.15 mN m^{-1} with air. The magnification and distance between the camera and the drop was calibrated against the diameter of the needle (0.6419 mm).

Dynamic light scattering (DLS)

DLS was conducted using a *Malvern Zetasizer Nano Series*, using either disposable plastic cuvettes for size, or folded capillary zeta cells for zeta potential. *Zetasizer* software was calibrated with constants from *poly*(styrene-*alt*-maleic acid) in PBS (50 mM, 0.2 M NaCl). Samples were diluted to a concentration of 0.1% (wt./v.), sufficient to assume an infinite dilution regime.

Prior to all measurements, solutions were passed through a 0.45 μm *Millex Millipore* membrane filter to remove contaminant scatters such as dust. Measurements were taking using backscattering (θ = 173°) and λ = 633 nm. All values reported relate to volume particle size distribution and in all cases five sets of measurements were taken, each with at least 12 runs, to ensure satisfactory cumulative fits.

Small angle neutron scattering (SANS). SANS was performed at the *ISIS Neutron and Muon Source* (Rutherford Appleton Laboratory, Didcot, UK), on the *Larmor* and *Zoom* instruments (**https://doi.org/10.5286/ISIS.E.RB1910182**), using 1 mm quartz *Hellma* cells at 25 °C.

Data were collected on Larmor using the standard configuration for rectangular quartz cuvettes. A wavelength band of 0.9 to 13.3 Å was used with apertures of 20 × 20 mm^2 and 6 × 8 mm^2 separated by a distance of 5.1 m. The sample to detector distance was 4.1 m with the detector consisting of 80, 600 mm long, position sensitive 8 mm diameter ^{3}He tube detectors. Prior to experiments, samples were mounted in a temperature controlled multi-position sample changer.

Data were collected on the Zoom SANS instrument in the standard configuration for rectangular quartz cuvettes, with a multi-position temperature controlled sample changer. A wavelength band of 1.75 to 16.5 Å was used with apertures of 20 × 20 mm^2 (A1) and 8 × 8 mm^2 (A2). The source to sample distance was set to 4.0 m, and the sample to detector distance was 4.0 m.

Data were subsequently reduced and the varying solution contrasts simultaneously fit (full description available in the ESI†). Copolymer aggregates were fit to either core shell spherical or cylindrical models (Fig. S7, ESI†), using the fixed parameters found in Table S6 (ESI†). Similarly, SMALP nanodiscs were fit to the core shell bicelle model outlined in Fig. 1b.

Results & discussion

Polymer synthesis & characterisation

The physical characteristics of the RAFT synthesised copolymers as well as, for comparison, a commercially available SMA2000 material (*Cray Valley*) are outlined in Table 1. The RAFT copolymer has, measured by GPC in THF relative to polystyrene standards, a molecular weight comparable with SMA2000 but a lower polydispersity (Fig. 3a). The 2 : 1 St : MAnh ratio was confirmed by ^{1}H NMR (Fig. S2, ESI†) and the poly((St-*alt*-MA)-*b*-St) block architecture by ^{13}C NMR (Fig. S3 – Full details in ESI†). Successful hydrolysis of SMAnh polymers to the corresponding maleic acid versions, coded here SMA-SC_{12}, was confirmed by loss of anhydride (~1854 cm^{-1} and 1773 cm^{-1}) and growth of acid (~1563 cm^{-1}) peaks in the FTIR spectra (Fig. S1 – Full details in ESI†), whereas those related to styrene were instead retained post hydrolysis. The same procedures were used to prepare partially deuterated materials (*d*-SMAnh) using d_6-styrene to expand the range of available contrasts for small angle neutron scattering (SANS) experiments. A further two copolymers, SMAnh-B and SMAnh-C, were also synthesised with a 2 : 1 composition, but with higher molecular weights, to investigate the effect of increasing the size of the styrene homoblock.

Modification of the end group of SMAnh followed the method of Chen *et al.*[27] Reaction with excess radical initiators,

Table 1 Characteristics of 2 : 1 SMAnh2000 and RAFT-synthesised SMAnh variants

Polymer	$M_{n(pre)}$/kDa[a]	Conversion/%	Comonomer ratio[b]	M_n/kDa[b]	PDI[b]	DP_n (Sty)[c]	DP_n (MAnh)[c]	Length styrene homoblock[d]
SMAnh2000	—	—	2 : 1	4.00	1.80	—	—	—
SMAnh	6.0	78.7	2 : 1	4.79	1.15	29	15	14
d-SMAnh	6.0	96.7	2 : 1	6.20	1.13	38	20	18
SMAnh (B)	8.0	88.0	2 : 1	5.47	1.15	33	17	16
SMAnh (C)	10.0	81.0	2 : 1	8.04	1.18	49	26	23

[a] $M_{n(pre)} = ((n_{(Sty)} \times M_{r(Sty)})/n_{(DDMAT)}) + ((n_{(MAnh)} \times M_{r(MAnh)})/n_{(DDMAT)}) + M_{r(DDMAT)})$. [b] Molecular weights (M_n) and polydispersity index (PDI) determined from GPC calibrated with narrow PDI polystyrene standard. [c] Degree of Polymerisation (DP_n) = $((M_n - M_{r\ (end\ groups)}) \times$ monomer ratio)/$M_{r(monomer)}$, with monomer ratio determined from ^{1}H NMR (Fig. S2, ESI). [d] Length of styrene homoblock = $DP_{n(Sty)} - DP_{n(MAnh)}$, assuming no semi-alternating regions given the lack of any semi-alternating peaks in ^{13}C NMR (Fig. S3, ESI).

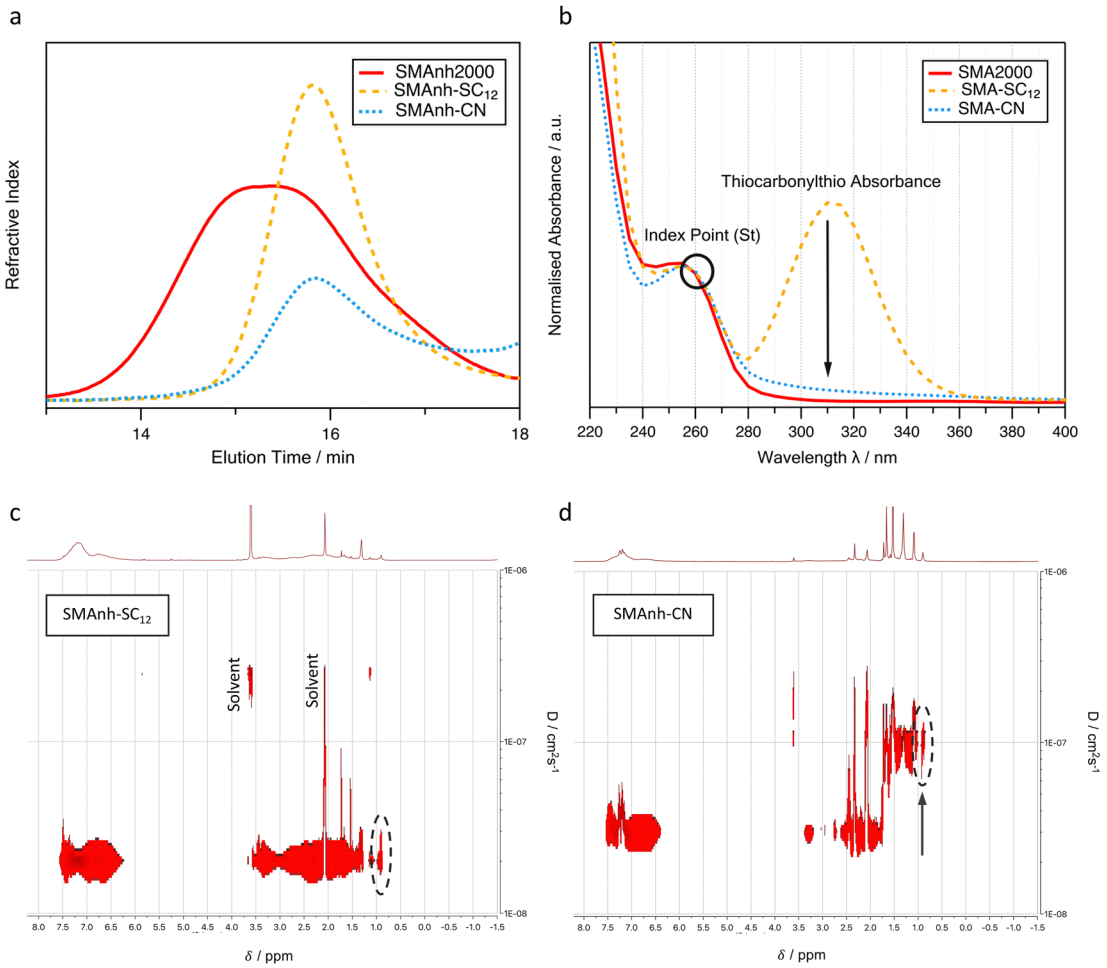

Fig. 3 (a) GPC chromatograms for SMAnh2000, SMAnh-SC_{12} and SMAnh-CN. (b) UV-vis spectra of SMA-SC_{12} and SMA-CN in PBS solutions normalised at styrene absorbance (260 nm) for comparison. (c-d) ^{1}H DOSY NMR spectra of (c) SMAnh-SC_{12} and (d) SMAnh-CN. Arrow indicates cleavage of thiocarbonylthio end group which diffuses at the rate of the copolymer in SMAnh-SC_{12}, and at the rate of the solvent in SMAnh-CN.

AIBN, and lauroyl peroxide replaced the alkylthiocarbonylthio end group from the RAFT agent with a less hydrophobic cyanoisopropropyl group (coded SMA-CN).

The characteristic yellow colour of the RAFT materials was lost during the reaction. UV-visible spectra (Fig. 3b), showed the loss of the thiocarbonylthio absorbance at 310 nm relative to styrene absorbance at 260 nm. From these data, an estimated 93% end group exchange efficiency was achieved compared with SMA2000 having no alkylthiocarbonylthio end group. Attempts were made to confirm the presence of cyanoisopropyl end groups in SMA-CN using ^{1}H-^{15}N HMBC NMR experiments (Fig. S4, ESI†). Tentatively, an additional nitrogen environment in comparison with SMA-SC_{12} was observed, however, assignment as a nitrile or amine was inconclusive. Cleavage of the alkylthiocarbonylthio groups was further confirmed by monitoring the peak at δ = 0.8[28] corresponding to the CH_3 unit terminating the SC_{12} chain in the ^{1}H DOSY NMR spectra (Fig. 3c) which diffused faster in SMAnh-CN samples.

The chain length distribution also remained monomodal in the GPC (Fig. 3a), an indication that no significant chain coupling occurred. Additionally, unidentified low molecular weight species gave rise to signals in the FTIR and ^{1}H NMR spectra for SMAnh-CN (Fig. S1 and S2, ESI†), but were removed on subsequent work up of the acid (SMA-CN) materials post hydrolysis.

Behaviour of copolymers in solution

Before examining their propensity for nanodisc formation, the behaviour of the copolymers alone in solution was examined. In aqueous solution at pH > 9, SMA has too high a charge density to bind to a membrane, while at pH < 6, the polymer is more hydrophobic and forms aggregates.[15] Speculation about the structures adopted by SMA in solution have led to suggestions that it is likely that aggregation occurs with styrene partitioned into a 'protected' core.[26,29,30] This is believed to be driven by hydrophobic styrene interactions in solutions of high ionic strength (>125 mM) to screen interchain repulsion, where copolymers enriched with styrene, such as those with homoblocks induced by RAFT, may form larger, more polydisperse aggregates.[30] This aggregation behaviour, as has been seen with detergents, is likely to influence SMALP self-assembly through the requirement for copolymer chains to dissociate from these aggregates prior to membrane disruption and nanodisc formation.[30,31]

Interfacial surface tension measurements of aqueous SMA solutions in PBS buffer at pH = 8.0 were measured against air (Fig. 4a) or dodecane (Fig. 4b), using pendant drop tensiometry (Fig. S5, ESI†). Dodecane was chosen to mimic the hydrophobic C_{12} chains of DMPC lipids, commonly used as the model membrane for testing SMALP formation. Measurements were taken at concentrations ranging from 0.02% to 1.65% (w/v), the highest concentration being that at which nanodiscs were prepared.

Each of the polymers reduces the surface tension of PBS measured against either an air or a dodecane interface up to concentrations around 0.4% (w/v), above which little further change occurs. SMA2000 showed the largest change in value as solution concentration increased, indicating the highest surface activity. At the PBS-air interface, the behaviour of SMA-CN is similar to that of SMA2000, while the presence of the dodecyltrithiocarbonyl end group in SMA-SC$_{12}$ reduces the surface activity. This is interesting as a greater surface activity would usually be expected from a more hydrophobic material. The results instead suggest the presence of solvated aggregates which have relatively low surface activity. Equilibrium may not have been reached during the timescale of the measurement, as it would be unfavorable for the more hydrophobic polymers to be free in solution and not to concentrate at the interface. When measured against dodecane, the random copolymer again showed the largest reduction in surface tension although there was less difference between the RAFT copolymers.

The corresponding dynamic light scattering results for SMA copolymer solutions in PBS at 25 °C (Fig. 5a and b) reveal that some degree of aggregation occurs even at concentrations as

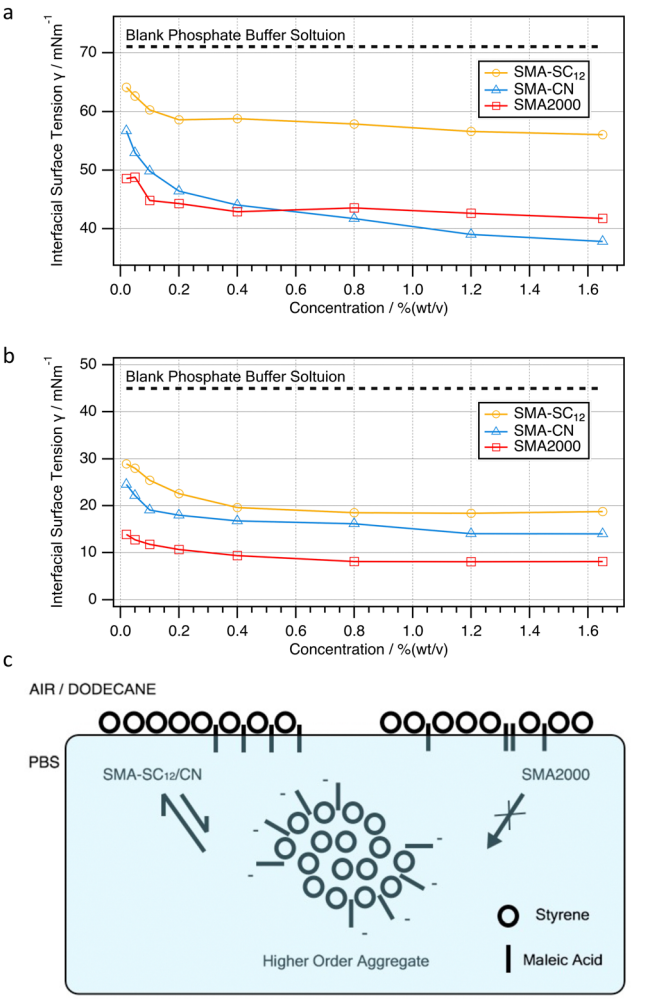

Fig. 4 Interfacial surface tension of SMA solutions (a) at air – PBS interface (b) at dodecane – PBS interface. Uncertainties were calculated taken from 10 s movie composed of 100 frames at 95% confidence interval but are smaller than data symbols. (c) Schematic representation of interfacial behaviour of SMA species in solution. Single chains tether to surface and reduce surface tension, whereas dissolved higher order aggregates remove polymer chains from this interface.

low as 0.02% (w/v) although the aggregates are small (~2–4 nm diameter) and likely composed of only two or three chains. As concentrations increase, SMA2000 aggregates only reached a size of around 4 nm, whereas RAFT copolymers formed larger aggregates, reaching a plateau around 12–13 nm at similar concentrations to where surface tension was minimised (0.2–0.4% (w/v)). The size of the aggregates of the two RAFT copolymers in solution were almost identical, suggesting that this is mainly influenced by the diblock structure and overall composition rather than by the end groups. This size possibly represents the maximum number of chains that can be accommodated before charge repulsion becomes too great. It is interesting to note that despite their different sizes, the zeta potentials (Table S3, ESI†) of the aggregates from all three copolymers, measured at a concentration of 1.2% (w/v), were almost identical: SMA2000, −24.9 ± 1.9 mV, SMA-SC$_{12}$, −24.8 ± 1.3 mV and SMA-CN, −24.7 ± 1.9 mV, implying that the surface

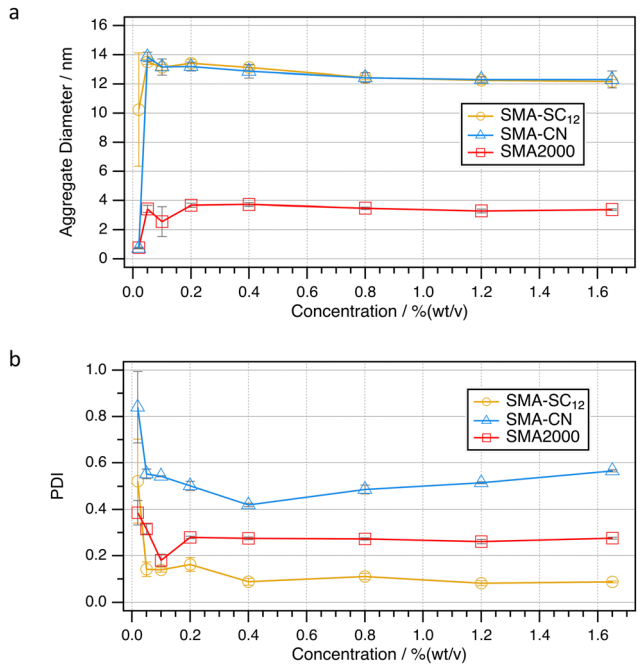

Fig. 5 DLS measurements of (a) SMA copolymer aggregate size in PBS solutions and (b) corresponding PDI values. Uncertainties reported at 95% CI from 5 sets of at least 12 measurements. Lines between points are a guide to the eye.

of the aggregate was similar across all materials. These data add further evidence that the RAFT aggregates consist of a polystyrene core surrounded by SMA.

These results can potentially be explained by the model illustrated schematically in Fig. 4c, where the system contains a mixture of single polymer chains adsorbed to the surface, which lower the surface tension, and copolymer aggregates in the bulk solution that remove chains from the interface.[27] The random architecture of SMA2000 does not provide a driving force for aggregate formation in solution, and hence allows the highest reduction in surface tension against air and dodecane at low concentrations (Fig. 3b and c). Both SMA-SC_{12} and SMA-CN have less effect on surface tension and the values plateau at higher values, consistent with the formation of aggregates as suggested by DLS. SMA-CN appears to be less susceptible to irreversible aggregate formation compared with SMA-SC_{12}, with greater surface adsorption resulting in a lower surface tension. This means that the polymers are more mobile, able to escape the aggregates on the experimental timescales, and this effect is more noticeable in air than dodecane. This is possibly due to the reduced ability of the hydrophobic styrene homoblock to insert into the styrene core of the aggregates due to being capped by the hydrophilic end group.

Heating the aggregate solutions provides further insight into their assembly. Using solutions of commercial SMA copolymers, Brady *et al.* found that those enriched in styrene *versus* maleic acid had a more pronounced effect in response to elevated temperatures.[30] It was found that supramolecular structures increased in size and polydispersity, attributed to styrene insertion, leading to the rationale that hydrophobic interactions are more dominant than hydrogen bonding in stabilising these aggregates. In this work, aggregates formed by SMA2000 indeed increased in size and polydispersity upon heating towards 45 °C, before collapsing slightly in size as 65 °C was reached (Table S4, ESI†). This effect was more marked at lower concentrations (0.02% (wt/v)) where aggregates had not yet reached their maximum size. Solutions of RAFT-made SMA-CN followed a similar trend of size with heating, again with a noticeable increase in polydispersity. Interestingly, solutions of SMA-SC_{12} saw a slight decrease in size accompanied by a large decrease in polydispersity upon heating. There was a consistent difference between SMA-CN and SMA-SC_{12}, highlighting the potentially potent influence of the homoblock end group. Du *et al.* found that assembly of hydrophilic RAFT polymers in solution was highly dependent on the identity of the end groups.[32] Despite accounting for a low volume fraction of the polymer, aggregation could be disrupted even by altering the hydrophobicity of an end group at only a single terminus.

It is unclear whether the effects seen here are due to the dominant interactions switching from hydrophobic to hydrophilic at higher temperatures, or whether styrene becomes more mobile (T_g SMA $\sim$ 70 °C) and kinetic effects are responsible. Regardless, we believe these results can be rationalised by styrene-enriched copolymer domains partitioning into the solvent-protected aggregate core. It may be that SMA-CN, with a more hydrophilic end group associated with the styrene homoblock, is sufficient to prevent effective insertion into the aggregate.

To further investigate the location and structure of the styrene homoblock, SANS data for these aggregates was also collected from a series of contrast-matched PBS solutions (Fig. 6a). For full experimental details, see Section 2.4 SANS in ESI.† Data were subsequently reduced in *Mantid* software[33] before the varying sample contrasts were simultaneously fitted using the *NIST* SANS Analysis package within *Igor Pro (Wavemetrics).*[34] Scattering data from SMA-SC_{12} aggregates (Fig. 6b) were best represented by a core–shell sphere model (Fig. S7, ESI†) with a polydisperse core radius.[35] Varying the ratio of H_2O to D_2O in the solvent allowed contrast matching of the scattering length density (SLD) of a d_6-styrene core and a 1 : 1 SMA shell, thus isolating the two structural components (Fig. 6a). Scattering from SMA-SC_{12} solutions fitted model aggregates that had a styrene core radius of 3.0 $\pm$ 1.0 nm, with a PDI of 0.28, and a shell thickness 1.1 $\pm$ 0.4 nm which was hydrated with 0.4 $\pm$ 0.1 mole fraction solvent.

SMA-CN aggregates were best fitted using a similar core–shell cylinder model (Fig. S7, ESI†), the greater aspect ratio of which was indicated by the shallower gradient observed at mid-q (Fig. 6c) (see Fig. S8 and Table S9 for example fitted to a spherical model, ESI†). Here, data corresponded to a core radius of 3.0 $\pm$ 1.0 nm, with a length of 1.5 $\pm$ 0.4 nm and PDI of 0.56 (in line with DLS results). These values could equally represent an oblate-type ellipsoid structure, such as that proposed by Brady *et al.* albeit using commercial copolymers,[30] but the high polydispersity found in fitting the SANS data (and also in DLS; Fig. 5b) makes it difficult to distinguish between ellipsoidal and

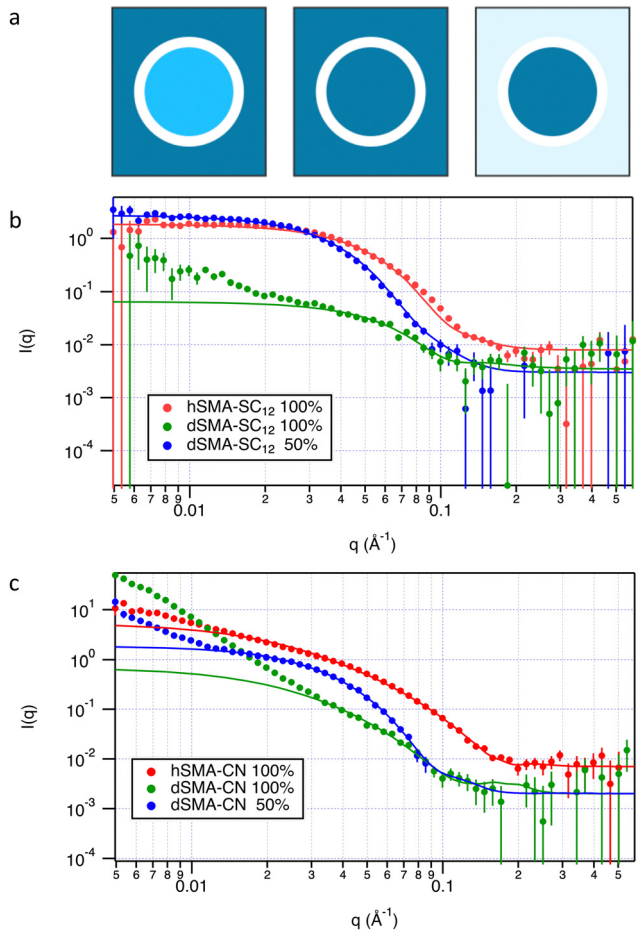

Fig. 6 (a) Representation of varying contrasts used to collect SANS data where (left to right) 100% D_2O and h-SMA examines the entire particle, 100% D_2O d-SMA emphasises the shell and 50% D_2O d-SMA emphasises the core. (b) SANS data for SMA-SC_{12} aggregates, fit to a core shell sphere model with polydisperse radius at various contrasts. (c) SANS data for SMA-CN aggregates, fit to a core shell cylinder model with polydisperse radius at various contrasts. The upturn at lower Q values also indicates the presence of larger, unfitted aggregates in this solution, particularly in the deuterated polymer solution. Full fit parameters can be found in Tables S7 and S8 (ESI†).

cylindrical models. These aggregates also had a comparatively thicker shell (1.5 ± 0.4 nm) that was less hydrated (0.15 ± 0.1), in accordance with the reduced insertion of styrene homoblocks into the core. Interestingly, if the CN end group is instead located in the shell, the average headgroup parameter would have also decreased, resulting in a more tightly packed polar region, providing packing parameters that would direct formation towards an oblate structure, as observed.

SMALP formation & structure

So, how do these properties influence the formation and structure of SMALPs? Nanodiscs were prepared using each of the copolymers using DMPC as a model phospholipid. Each of them successfully formed SMALPs under the usual conditions (25 °C; pH = 8.0; 1.65% wt polymer to 0.55% wt DMPC). DLS measurements showed the nanodisc diameters with DMPC to be 18.9 nm ± 1.0 nm, 14.86 nm ± 0.24 nm and 5.92 nm ± 0.11 nm, with SMA-SC_{12}, SMA-CN and SMA2000, respectively. The size order matches the corresponding surface tensions of the copolymer solutions against dodecane (Fig. 4b). This makes sense, as SMA-SC_{12} does not lower the interfacial tensions as much as the others, it should form larger discs, whereas the other polymers absorb more effectively to the lipid patch, lowering interfacial tension so that discs can be smaller. Polydispersities of the nanodiscs from the two RAFT copolymers were similar (0.45–0.48) whereas SMA2000 appeared to produce much more monodisperse discs (0.27). Similar sizes were found when using the deuterated copolymers, (r = 18.5 ± 0.5 nm, PDI = 0.52 ± 0.01 for dSMA-SC_{12} while r = 18.0 ± 0.8 nm, PDI = 0.43 ± 0.01 for dSMA-CN, both at 25 °C) albeit that they have slightly different molecular weights which is not expected to significantly influence nanodisc sizes.[13,18]

As was seen for SMA-SC_{12} aggregates, increasing the temperature to 65 °C caused the SMA-SC_{12} nanodiscs to decrease in both size and PDI (Table S5, ESI†) to radii of 11.2 ± 1.6 nm, PDI = 0.25 ± 0.01, compared with SMA-CN at the same temperature: 12.74 ± 0.44 nm, PDI = 0.44 ± 0.01. SMA2000 also contracted from 5.92 ± 0.11 nm to 4.91 ± 0.19 nm, PDI = 0.19 ± 0.05. As has been suggested in the literature by Hall *et al.*[22] and Lorigan and coworkers[24] these results indicate that SMA-SC_{12} is able to stabilise nanodiscs by insertion of the styrene homoblock and therefore, also the relatively large hydrophobic end group, into the lipid fragment of nanodiscs. Whilst this may provide additional stabilisation in comparison to SMA-CN, an inserted homoblock could also easily threaten the structural integrity of MPs encapsulated in these nanodiscs. For example, as shown in Table 2, incorporation of the model MP gramicidin into SMA-SC_{12} nanodiscs increased the diameter slightly to 22.48 ± 0.31 nm, whereas those from SMA-CN increased by a greater extent to 30.43 ± 0.96 nm. Both nanodisc species had a PDI of 0.25 ± 0.01 at 25 °C. Although the SC_{12} terminated homoblock may have stabilised the nanodiscs by inserting into the core, the exterior of gramicidin is also hydrophobic and these units would likely interact given their proximity. Interestingly, inclusion of gramicidin made no difference to the size of nanodiscs formed with SMA2000.

Table 2 SMALP nanodisc diameters from DLS measurements at 25 °C with DMPC lipid

Nanodisc sample	Lipid species	Diameter/nm[a]	PDI[a]
SMA-SC_{12}	DMPC	18.9 ± 1.0	0.48 ± 0.01
SMA-CN	DMPC	14.86 ± 0.24	0.45 ± 0.01
SMA2000	DMPC	5.92 ± 0.11	0.27 ± 0.02
SMA-SC_{12}	DMPC + gramicidin	22.48 ± 0.31	0.25 ± 0.01
SMA-CN	DMPC + gramicidin	30.43 ± 0.96	0.25 ± 0.01
SMA2000	DMPC + gramicidin	5.86 ± 0.17	0.50 ± 0.01
SMA-SC_{12} (B)	DMPC	18.69 ± 0.13	0.17 ± 0.01
SMA-SC_{12} (C)	DMPC	20.71 ± 0.82	0.18 ± 0.01
SMA-CN (B)	DMPC	16.34 ± 0.72	0.61 ± 0.02
SMA-CN (C)	DMPC	15.75 ± 0.61	0.58 ± 0.01

[a] Uncertainty at 95% confidence averaged from 5 sets of at least 12 scans.

To examine this further, SANS data from the nanodiscs formed with DMPC lipids were acquired. Here, data were fitted using a SMALP model based on a core–shell bicelle,[35] where the core and shell SLDs had been adapted to include the percentage polymer insertion and hydration, respectively, as separate fit parameters (Fig. 1b). Full details can be found in Section 2.4 SANS in the ESI.† A difference in behaviour between SMA-SC_{12} and SMA-CN is readily apparent (Fig. 7a and b), where at low-q ($q < 0.015$) the data undergo a step-change into a steeper gradient that could not be fitted, indicative of a greater extent of aggregation in this system. This difference between SMA-SC_{12} and SMA-CN persisted with increasing molecular weight and homoblock length, as seen by comparing the data from polymers in Table 1: SMA-SC_{12} (B) and (C) *versus* SMA-CN (B) and (C), Fig. S10 and S11 (ESI†), respectively.

Taken together with data from the deuterated copolymers (Tables S10–S13 and Fig. S9a, b, ESI†), other trends between samples can be observed. SMA-SC_{12} nanodiscs fitted a radius between 3.4–4.4 nm, lipid core length 2.9–3.0 nm with a PDI of 0.20–0.29, and SMA-CN discs a radius between 3.8–4.1, lipid core length 3.3–3.4 nm with a PDI of 0.33–0.46. Hence, SMA-CN nanodiscs were on average thicker and more polydisperse. Whilst similar rim hydrations were found between the samples (~29–33%), SMA-CN nanodiscs were also found to incorporate less polymer into the lipid tail core (20–24%) *versus* SMA-SC_{12} (26–31%). These results align with the findings from the polymer-only aggregates, that capping the styrene homoblock with a hydrophilic group may hinder insertion of the block into hydrophobic regions during assembly, generating more disperse structures. The inability of the styrene homoblock to insert and be shielded from the polar solvent may also be the reason for the greater extent of aggregation seen in the scattering from these samples, and also the larger impact upon surface tension as the extended copolymer adsorbs to the interface to a greater extent.

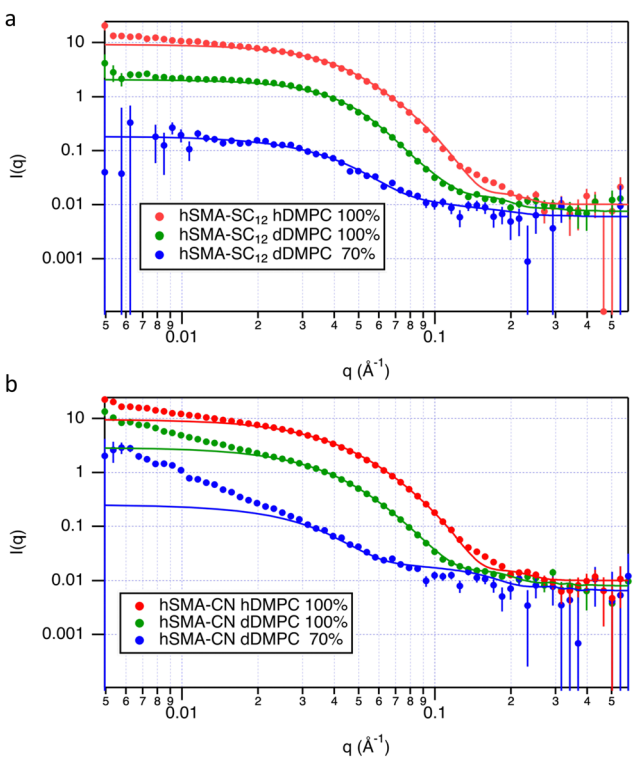

Fig. 7 SANS data for (a) SMA-SC_{12} and (b) SMA-CN nanodiscs with hDMPC and dDMPC at various contrasts fit to SMALP model based on a core–shell bicelle. Full fit parameters can be found in Tables S10 and S12 (ESI†).

Data from polymers with higher molecular weights, SMA (B) and SMA (C), add to these conclusions (Tables S14–S17, ESI†). Increasing the molecular weight, and hence length of the styrene homoblocks, caused SMA-SC_{12} nanodiscs to get progressively thicker (lipid core lengths from 3.3 (± 0.3) to 3.8 (± 0.2) nm), wider (4.5 (± 0.5) to 4.9 (± 0.6) nm), and somewhat more polydisperse (0.26 (± 0.04) to 0.31 (±0.04)). Rim thickness also appeared to slightly decrease (0.9 (± 0.4) to 0.8 (± 0.4) nm), and the percentage polymer in the core increased (26 (± 7) to 35 (± 6) %), in line with greater penetration of the homoblock into the nanodisc cores. Although this interpretation should be treated cautiously, due to the number of variables involved, nanodiscs prepared using SMA-CN (B) and (C) did not significantly vary with increasing polymer molecular weight, with the scattering data instead fitting to models within error of the parameters previously used.

Interestingly, SMA-SC_{12} did not solubilise DPPC lipids using the same procedure as for DMPC, instead producing large 88 ± 38 nm diameter structures without loss of turbidity implying the existence of aggregates outside the range of DLS measurements (Table S5 and Fig. S6, ESI†). This lipid has an acyl chain only two carbons longer than DMPC, but a much increased gel transition temperature ($T_{g,DMPC}$ = 24 °C; $T_{g,DPPC}$ = 41 °C).[36] This means that, at the temperature of SMALP formation (25 °C), whereas DMPC is a liquid, DPPC chains are frozen, making it harder to incorporate other species into the bilayer. However, SMA-CN and SMA2000, could successfully incorporate DPPC lipids into nanodiscs, similar in dimension to those formed with DMPC. This further suggests that penetration of SMA-SC_{12} into the lipid-tail region in the nanodisc cores is required for this polymer to form nanodiscs. It is possible that, as SMA-CN and SMA2000 absorb effectively to the PBS:dodecane interface, only a few styrene units are needed to interact with the edges of the solid lipid tails to lower interfacial tension for these species to form nanodiscs, opposed to SMA-SC_{12} which relies on disrupting the packing of the lipid phase through insertion. This serves to highlight that large differences in SMALP and aggregate behaviour can be achieved by modifying only a relatively minor unit along the greater copolymer chain.

Conclusions

Well defined styrene-maleic acid copolymers have been synthesised by RAFT polymerisation and characterised by gel permeation chromatography, UV-vis and NMR spectroscopies. Copolymers prepared by RAFT have a hydrophobic -SC_{12} end group. To investigate its effect upon nanodisc formation, the end group

was efficiently cleaved by reaction with excess radical initiators without inducing chain combination.

Surface tension measurements showed that the RAFT copolymers were less surface active than a pseudo-random commercially available copolymer of similar molecular weight, one reason being that they form kinetically-trapped aggregates in aqueous solution, reducing the amount of material available for interfacial adsorption. Replacement of the hydrophobic end group with a more hydrophilic -CN group slightly lowered the surface tension but did not significantly change the aggregate size or zeta potential. Further mechanistic information was obtained from neutron scattering studies, facilitated by the synthesis of copolymers from deuterated styrene. SANS data from SMA-SC_{12} and SMA-CN aggregates fitted a core shell sphere and cylinder model, respectively. These results add further support to the accepted model of copolymer aggregation around a solvent-protected styrenic core and that dissociation from this is first needed for interfacial interaction. The presence of more hydrophilic end groups somewhat disrupted copolymer aggregation due to the reduced ability of styrene homoblocks, terminated by a hydrophilic end group, to insert into aggregate cores but which are instead free to diffuse into solution. This model is consistent with the DLS data which also showed that raising the temperature stabilised SMA-SC_{12} aggregates whilst having a disruptive effect upon SMA-CN and SMA2000 macrostructures.

SMALP nanodiscs were formed from all the copolymers using DMPC as a model lipid. Those with the highest surface activity produced the smallest nanodiscs. This is in line with colloidal theory, where reduced surface tension allows smaller objects to be more stable in solution, and could possibly be used as a predictive metric for disc formation in future. Structural analysis of the resultant discs suggested that styrene homoblocks were adsorbing onto the lipid fragment of nanodiscs and that this was the driver of nanodisc self-assembly. SMA-CN showed less insertion into the nanodisc core than SMA-SC_{12}, and SMA-SC_{12} nanodiscs instead grew longer with increasing homoblock lengths as the styrene component was incorporated into the DMPC bilayer, rather than only interacting with the lipids at the edge of the bilayer. This could have consequences for those wishing to use SMA-SC_{12} for MP extraction, as it is likely this will perturb MP structure or dynamics to at least some degree. Hence, the novel variant, SMA-CN, presents a potential advantage by inhibiting styrene homoblock insertion into the nanodisc core alleviating any possible interference with the MP structure or dynamics. Ultimately, the usefulness of these block copolymers depends on their ability to solubilize membrane proteins. While this has been shown to be feasible for gramicidin as a model, differences have been revealed in the nanodisc structures formed. Further work is underway to more completely characterise their performance in real membrane systems.

SMA-SC_{12} did not solubilise the longer lipid species, DPPC, at room temperature. As DPPC was below T_g during SMALP formation, it is likely that the copolymer could not penetrate the solid bilayer to disrupt lipid packing. In comparison, SMA-CN and SMA2000 did solubilise DPPC. Effective at lowering the interfacial tension at the PBS:dodecane interface, it is possible these polymers do not need to insert into the bilayer and instead only a few styrene units interact with the edge of the lipid tails to produce discs. This serves to highlight the potential behavioural differences in SMA aggregate and nanodisc structures that can be prompted even by subtle alterations to the copolymer chain, influencing their activity with different lipid species and phases.

The work demonstrates that in addition to the global architecture of the copolymer, changing the chain end groups can significantly affect how the copolymer blocks work in conjunction to achieve membrane solubilisation. Systematic investigation of SMA (and other copolymer) end groups may lead to the discovery of yet further influences upon nanodisc behaviour, especially when used alongside controlled polymerisation.

Author contributions

The manuscript was written through contributions of all authors. GMN: investigation, writing – original draft, writing – review & editing; KAM: SANS investigation; ERS: copolymer synthesis of SMA-SC_{12}/CN (B) and SMA-SC_{12}/CN (C) JD: SANS investigation; RD: SANS investigation; GJP: conceptualisation, methodology, supervision, writing – review & editing; KJE: SANS investigation, conceptualisation, funding acquisition, supervision, writing – review & editing. All authors have given approval to the final version of the manuscript.

Conflicts of interest

There are no conflicts to declare.

Acknowledgements

Gratitude is extended to Dr John Lowe of the Materials Characterisation (MC^2) facility at the University of Bath, for assistance with DOSY and HMBC spectroscopy. GMN and KAM acknowledge funding from the EPSRC Centre for Doctoral Training in Sustainable Chemical Technologies, EPSRC Grant EP/L016354/1. KAM further acknowledges funding from ISIS Neutron and Muon Source (STFC Studentship Agreement #SA-54). We thank ISIS Neutron and Muon Source for provision of beamtime on Larmor and ZOOM under allocation RB1910182. Raw data (**https://doi.org/10.5286/ISIS.E.RB1910182**) collected on Lamor can be found in the ISIS-ICAT system at **https://data.isis.stfc.ac.uk/browse/instrument/57054346/facilityCycle/87730662/investigation/101134497/dataset/102423987**, and those collected on ZOOM at **https://data.isis.stfc.ac.uk/browse/instrument/57054085/facilityCycle/87730662/investigation/102490405/dataset/102763354**. Data supporting this manuscript can be downloaded from the University of Bath Research Data Archive: **https://doi.org/10.15125/BATH-01291**.

References

1 M. S. Almén, K. J. V. Nordström, R. Fredriksson and H. B. Schiöth, Mapping the human membrane proteome:

a majority of the human membrane proteins can be classified according to function and evolutionary origin, *BMC Biol.*, 2009, **7**, 50.

2 J. P. Overington, B. Al-Lazikani and A. L. Hopkins, How many drug targets are there?, *Nat. Rev. Drug Discovery*, 2006, **5**, 993–996.

3 A. Roy, Membrane Preparation and Solubilization, *Methods Enzymol.*, 2015, **557**, 45–56.

4 Z. Stroud, S. C. L. Hall and T. R. Dafforn, Purification of membrane proteins free from conventional detergents: SMA, new polymers, new opportunities and new insights, *Methods*, 2018, **147**, 106–117.

5 A. M. Seddon, P. Curnow and P. J. Booth, Membrane proteins, lipids and detergents: not just a soap opera, *Biochim. Biophys. Acta, Biomembr.*, 1666, **2004**, 105–117.

6 J. M. Dörr, S. Scheidelaar, M. C. Koorengevel, J. J. Dominguez, M. Schäfer, C. A. van Walree and J. A. Killian, The styrene–maleic acid copolymer: a versatile tool in membrane research, *Eur. Biophys. J.*, 2016, **45**, 3–21.

7 S. M. Smith, *Strategies for the Purification of Membrane Proteins. in Protein Chromatography*, ed. Walls, D. & Loughran, S. T., 2011, vol. 681, pp. 485–496.

8 T. Arnold and D. Linke, in The Use of Detergents to Purify Membrane Proteins, *Current Protocols in Protein Science*, ed. Coligan, J. E., Dunn, B. M., Speicher, D. W. & Wingfield, P. T., John Wiley & Sons, Inc, 2008.

9 M. Zoonens, F. Zito, K. L. Martinez and J. L. Popot, in *Membrane Proteins Production for Structural Analysis*, ed. I. Mus-Veteau, Springer, New York, 2014, pp. 173-203.

10 T. H. Bayburt, Y. V. Grinkova and S. G. Sligar, Self-Assembly of Discoidal Phospholipid Bilayer Nanoparticles with Membrane Scaffold Proteins, *Nano Lett.*, 2002, **2**, 853–856.

11 T. J. Knowles, R. Finka, C. Smith, Y. P. Lin, T. Dafforn and M. Overduin, Membrane Proteins Solubilized Intact in Lipid Containing Nanoparticles Bounded by Styrene Maleic Acid Copolymer, *J. Am. Chem. Soc.*, 2009, **131**, 7484–7485.

12 M. Jamshad, V. Grimard, I. Idini, T. J. Knowles, M. R. Dowle, N. Schofield, P. Sridhar, Y. Lin, R. Finka, M. Wheatley, O. R. T. Thomas, R. Palmer, M. Overduin, C. Govaerts, J. Ruysschaert, K. J. Edler and T. J. Dafforn, Structural analysis of a nanoparticle containing a lipid bilayer used for detergent-free extraction of membrane proteins, *Nano Res.*, 2015, **8**, 774–789.

13 M. Overduin and B. Klumperman, Advancing membrane biology with poly(styrene-*co*-maleic acid)-based native nanodiscs, *Eur. Polym. J.*, 2019, **110**, 63–68.

14 S. Scheidelaar, M. C. Koorengevel, J. D. Pardo, J. D. Meeldijk, E. Breukink and J. A. Killian, Molecular model for the solubilization of membranes into nanodisks by styrene maleic acid copolymers, *Biophys. J.*, 2015, **108**, 279–290.

15 S. Scheidelaar, M. V. Koorengevel, C. A. van Walree, J. J. Dominguez, J. M. Dörr and J. A. Killian, Effect of polymer composition and pH on membrane solubilization by styrene-maleic acid copolymers, *Biophys. J.*, 2016, **111**, 1974–1986.

16 B. Klumperman, Mechanistic considerations on styrene–maleic anhydride copolymerization reactions, *Polym. Chem.*, 2010, **1**, 558–562.

17 A. H. Kopfa, C. Martijn, C. Koorengevela, C. A. van Walreea, T. R. Dafforn and J. A. Killiana, A simple and convenient method for the hydrolysis of styrene-maleic anhydride copolymers to styrene-maleic acid copolymers, *Chem. Phys. Lipids*, 2019, **218**, 85–90.

18 T. Ravulaa, N. Z. Hardin and A. Ramamoorthy, Polymer nanodiscs: Advantages and limitations, *Chem. Phys. Lipids*, 2019, **219**, 45–49.

19 A. O. Oluwole, B. Danielczak, A. Meister, J. O. Babalola, C. Vargas and S. Keller, Solubilization of Membrane Proteins into Functional Lipid-Bilayer Nanodiscs Using a Diisobutylene/Maleic Acid Copolymer, *Angew. Chem., Int. Ed.*, 2017, **56**(7), 1919–1924.

20 S. C. L. Hall, C. Tognoloni, J. Charlton, É. C. Bragginton, A. J. Rothnie, P. Sridhar, M. Wheatley, T. J. Knowles, T. Arnold and K. J. Edler, *et al.*, An acid-compatible co-polymer for the solubilization of membranes and proteins into lipid bilayer-containing nanoparticles, *Nanoscale*, 2018, **10**, 10609–10619.

21 P. S. Orekhov, M. E. Bozdaganyan, N. Voskoboynikova, A. Y. Mulkidjanian, M. G. Karlova, A. Yudenko, A. Remeeva, Y. L. Ryzhykau, I. Gushchin and V. I. Gordeliy, *et al.*, Mechanisms of Formation, Structure, and Dynamics of Lipoprotein Discs Stabilized by Amphiphilic Copolymers: A Comprehensive Review, *Nanomaterials*, 2022, **12**(3), 361.

22 S. C. Hall, C. Tognoloni, G. J. Price, B. Klumperman, K. J. Edler, T. R. Dafforn and T. Arnold, The influence of polymer structure on the properties and self-assembly of SMALPs, *Biomacromolecules*, 2018, **19**, 761–772.

23 B. D. Harding, G. Dixit, K. M. Burridge, I. D. Sahu, C. Dabney-Smith, R. E. Edelmann, D. Konkolewicz and G. A. Lorigan, Characterizing the structure of styrene-maleic acid copolymer-lipid nanoparticles (SMALPs) using RAFT polymerization for membrane protein spectroscopic studies, *Chem. Phys. Lipids*, 2019, **218**, 65–72.

24 A. F. Craig, E. E. Clark, I. D. Sahu, R. Zhang, N. D. Frantz, M. S. Al-Abdul-Wahid, C. Dabney-Smith, D. Konkolewicz and G. A. Lorigan, Tuning the size of styrene-maleic acid copolymer-lipid nanoparticles (SMALPs) using RAFT polymerization for biophysical studies, *Biochem. Biophys. Acta*, 2016, **1858**, 2931–2939.

25 B. Klumperman, Iterative RAFT-Mediated Copolymerization of Styrene and Maleic Anhydride toward Sequence- and Length-Controlled Copolymers and Their Applications for Solubilizing Lipid Membranes, *Biomacromolecules*, 2020, **21**, 3287–3300.

26 S. Harrisson and K. L. Wooley, Shell-crosslinked nanostructures from amphiphilic AB and ABA block copolymers of styrene-*alt*-(maleic anhydride) and styrene: polymerization, assembly and stabilization in one pot, *Chem. Commun.*, 2005, 3259–3261.

27 M. Chen, G. Moad and E. Rizzardo, Thiocarbonylthio end group removal from RAFT-synthesized polymers by a radical-induced process, *J. Polym. Sci., Part A: Polym. Chem.*, 2009, **47**, 6704–6714.

28 O. O. Oyeneye, W. Z. Xu and P. A. Charpentier, Adhesive RAFT agents for controlled polymerization of acrylamide: effect of catechol-end R groups, *RSC Adv.*, 2015, **5**, 76919–76926.
29 G. Garnier, M. Duskova-Smrckova, R. Vyhnalkova, T. Van de Ven and J.-F. Revol, Association in Solution and Adsorption at an Air−Water Interface of Alternating Copolymers of Maleic Anhydride and Styrene, *Langmuir*, 2000, **16**, 3757–3763.
30 N. G. Brady, S. Qian and B. D. Bruce, Analysis of styrene maleic acid alternating copolymer supramolecular assemblies in solution by small angle X-ray scattering, *Europ. Poly. J.*, 2019, **111**, 178–184.
31 P. S. Orekhov, M. E. Bozdaganyan, N. Voskoboynikova, A. Y. Mulkidjanian, H.-J. Steinhoff and K. V. Shaitan, Styrene/Maleic Acid Copolymers Form SMALPs by Pulling Lipid Patches out of the Lipid Bilayer, *Langmuir*, 2019, **35**, 3748–3758.
32 J. Du, H. Willcock, J. P. Patterson, I. Portman and R. K. O'Reilly, Self-assembly of hydrophilic homopolymers: a matter of RAFT end groups, *Small*, 2011, **7**, 2070–2080.
33 O. Arnold, J. C. Bilheux, J. M. Borreguero, A. Buts, S. I. Campbell, L. Chapon, M. Doucet, N. Draper, R. Ferraz Leal, M. A. Gigg, V. E. Lynch, A. Markvardsen, D. J. Mikkelson, R. L. Mikkelson, R. Miller, K. Palmen, P. Parker, G. Passos, T. G. Perring, P. F. Peterson, S. Ren, M. A. Reuter, A. T. Savici, J. W. Taylor, R. J. Taylor, R. Tolchenov, W. Zhou and J. Zikovsky, *Nucl. Instrum. Methods Phys. Res., Sect. A*, 2014, **764**, 156–166.
34 S. R. Kline, *J. Appl. Crystallogr.*, 2006, **39**, 895–900.
35 A. Guinier and G. Fournet, *Small-angle scattering of X-rays*, John Wiley and Sons, New York, 1955.
36 L. Fernandez-Puente, I. Bivasm, M. D. Mitov and P. Méléard, Temperature and Chain Length Effects on Bending Elasticity of Phosphatidylcholine Bilayers, *EPL*, 1994, **28**, 181.

